Regular Article - Experimental Physics

Quartic gauge couplings and the radiation zero in pp → l±νγγ events at the LHC

P.J. Bell[a]

The University of Manchester, Oxford Road, Manchester M13 9PL, UK

Abstract We report a study of the process pp → l±νγγ at CERN's Large Hadron Collider, using a leading order partonic-level event generator interfaced to the Pythia program for showering and hadronisation and a with a generic detector simulation. The process is sensitive to possible anomalous quartic gauge boson couplings of the form WWγγ. It is shown how unitarity-safe limits may be placed on these anomalous couplings by applying a binned maximum likelihood fit to the distribution of the two-photon invariant mass, $M_{\gamma\gamma}$, below a cutoff of ∼1 TeV. Assuming 30 fb^{-1} of integrated luminosity, the expected limits are two orders of magnitude tighter than those available from LEP. It is also demonstrated how the Standard Model radiation zero feature of the qq̄′ → Wγγ process may be observed in the difference between the two-photon and charged lepton pseudo-rapidities.

PACS 14.70.Bh · 14.70.Fm

1 Introduction

In the Standard Model (SM) the form and strength of the self-interactions of the boson fields are specified by the SU(2) × U(1) gauge invariant form of the electroweak sector, through the $-\frac{1}{4}\mathbf{W}_{\mu\nu} \cdot \mathbf{W}^{\mu\nu}$ Lagrangian term. Any deviations in the self-couplings from their SM expectations may signal the presence of new physics at as yet unprobed energy scales: terms equivalent to anomalous gauge couplings may parametrise the low energy effects of the unknown new physics.

Whilst both anomalous triple and quartic gauge couplings offer an important test of the non-Abelian structure of the SM, the anomalous quartic gauge couplings (AQGCs) are also connected to the electroweak symmetry breaking sector; the WWWW quartic coupling must conspire with the Higgs to ensure good high energy behaviour in WW scattering. It has therefore been suggested that the AQGCs may provide a unique window on the mechanism responsible for the symmetry breaking, with any deviations from the SM expected behaviour being a potential sign of some alternative mechanism to that of the Higgs [1, 2].

Possible anomalous triple and quartic gauge couplings may be accessed through di- or tri-vector boson production processes, respectively, but the latter have so far attracted little interest given the modest event rates expected even at the LHC. The process qq̄′ → Wγγ, which is sensitive to the WWγγ four-point vertex, represents an obvious starting point to look for a tri-boson signal. Compared to those involving a higher number of heavy bosons, this process requires a relatively low partonic centre of mass energy and gives rise to clean leptonic final states suppressed by the branching of only one massive vector boson. It can be assumed that any deviations in the couplings from their SM expectation at the WWγγ vertex could be indicative of some general discrepancy in the quartic couplings sector, including the phenomenologically more interesting WWWW case.

Beyond providing a means of studying the AQGCs, Wγγ production itself is of interest for several other reasons. As in the qq̄′ → Wγ case, the process qq̄′ → Wγγ contains a so called *radiation zero* in its amplitude, the observation of which would provide another consistency check of the SM. In addition, W plus two-photon events will need to be considered when making high precision measurements of the W mass. Finally, Wγγ production is an irreducible background to the important H → γγ channel at the LHC.

The main objective of this work has been to evaluate the expected event rate for pp → l±νγγ (l = e, μ) at the LHC and investigate the sensitivity of this process to possible anomalous contributions to the WWγγ vertex. The theoretical framework for these AQGCs is outlined in section two. The SM expectations from previous Monte Carlo (MC) studies at the Tevatron and LHC are compared in section

[a] e-mail: paul.bell@cern.ch

three, where the adaptation of a generator for use in conjunction with a showering and hadronisation programme is also described. In section four, a binned maximum likelihood method is used to place limits on the AQGCs and these expected experimental limits are compared to those obtained from unitarity considerations. The possible observation of the radiation zero is described in the final section.

2 General formalism for anomalous quartic gauge couplings

The formalism for possible anomalous terms generating quartic gauge boson self-couplings has been widely discussed in the literature [1–4]. In the parametrisation first introduced in [2], the two lowest dimension effective Lagrangian terms that give rise to purely quartic couplings involving at least two photons are:

$$\mathcal{L}_6^0 = -\frac{e^2 \beta_0}{16} F_{\mu\nu} F^{\mu\nu} \boldsymbol{W}^{\alpha} \cdot \boldsymbol{W}_{\alpha},$$

$$\mathcal{L}_6^c = -\frac{e^2 \beta_c}{16} F_{\mu\alpha} F^{\mu\beta} \boldsymbol{W}^{\alpha} \cdot \boldsymbol{W}_{\beta}.$$

These are C and P conserving and are obtained by imposing local $U(1)_{em}$ gauge symmetry whilst also requiring the global custodial $SU(2)_c$ symmetry that constrains the electroweak parameter $\rho = 1$. Noting that the custodial $SU(2)_c$ field vector is

$$\boldsymbol{W}_{\alpha} = \begin{pmatrix} \frac{1}{\sqrt{2}}(W_{\alpha}^+ + W_{\alpha}^-) \\ \frac{i}{\sqrt{2}}(W_{\alpha}^+ - W_{\alpha}^-) \\ Z_{\alpha}/\cos\theta_W \end{pmatrix}$$

and identifying

$$\boldsymbol{W}_{\alpha} \cdot \boldsymbol{W}_{\beta} \rightarrow 2\left(W_{\alpha}^+ W_{\beta}^- + \frac{1}{2\cos^2\theta_W} Z_{\alpha} Z_{\beta} \right),$$
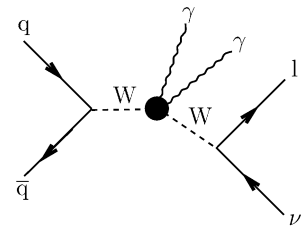
then in terms of the physical fields:

$$\mathcal{L}_6^0 = -\frac{e^2 \beta_0^W}{8} F_{\mu\nu} F^{\mu\nu} W^{+\alpha} W_{\alpha}^-$$
$$\quad - \frac{e^2 \beta_0^Z}{16\cos^2\theta_W} F_{\mu\nu} F^{\mu\nu} Z^{\alpha} Z_{\alpha},$$

$$\mathcal{L}_6^c = -\frac{e^2 \beta_c^W}{16} F_{\mu\alpha} F^{\mu\beta} \left(W^{+\alpha} W_{\beta}^- + W^{-\alpha} W_{\beta}^+ \right)$$
$$\quad - \frac{e^2 \beta_c^Z}{16\cos^2\theta_W} F_{\mu\alpha} F^{\mu\beta} Z^{\alpha} Z_{\beta}.$$

Thus, both terms generate AQGCs of the form $WW\gamma\gamma$ and $ZZ\gamma\gamma$. The parameters β_0 and β_c are distinguished here

Fig. 1 The contribution of the $WW\gamma\gamma$ vertex, which may receive an anomalous contribution governed by the coupling parameters β_0^W and β_c^W, to the process $q\bar{q}' \rightarrow l^{\pm}\nu\gamma\gamma$

for the W and Z vertices to comply with previous experimental measurements in which the couplings were studied independently [5]. Figure 1 shows how the process $q\bar{q}' \rightarrow l^{\pm}\nu\gamma\gamma$ includes a contribution from the $WW\gamma\gamma$ vertex and is thus sensitive to β_0^W and β_c^W.

Through the $F_{\mu\alpha} F^{\mu\beta}$ terms in the effective Lagrangians, the anomalous couplings will scale with the square of the photon energies, so a substantial improvement in the sensitivity can be expected at the LHC over the results from LEP.

3 Monte Carlo generation of $W\gamma\gamma$ events

3.1 Comparison of programmes and published results

Previous studies have been made of both $pp \rightarrow l\nu\gamma\gamma$ at the LHC by Éboli, Gonzalez-García, Lietti and Novaes [6] and $p\bar{p} \rightarrow l\nu\gamma\gamma$ at the Tevatron by Baur, Han, Kauer, Sobey and Zeppenfeld [7]. The MC programme used in these works have been obtained from the corresponding authors, and are referred to here as the Lietti and Baur MCs, respectively; they are described fully in the corresponding publications. Both programmes are based on Madgraph-generated amplitudes [8] that take into account all leading order diagrams for the $l^{\pm}\nu\gamma\gamma$ final state. Finite W width effects are included and all partons are assumed to be massless. Both programmes produce weighted events, the Lietti MC relying on Vegas [9] for the phase space integration and the Baur code making use of a custom three body phase space generator. The important difference between the programmes is that, whereas the Baur MC generates only SM events, the Lietti code includes the AQGC contribution to the $WW\gamma\gamma$ vertex, parametrised by the β_0 and β_c parameters.

Whilst the Lietti programme forms the basis of the work reported here, it is prudent to first compare the SM expectations from the two generators in order to validate the programmes and our usage of them. The generator-level cuts applied in order to approximately simulate the detector acceptance in the previous studies are summarised in Table 1. For the Tevatron (Baur MC), only the $W^- \rightarrow e^-\nu$ channel was considered, the W^+ channel not being implemented in the MC. At the LHC (Lietti MC) the complete $W^{\pm} \rightarrow l^{\pm}\nu$ ($l = e, \mu$) final state was studied. The MRS (A) and MRS (G) sets of proton structure functions were used for the Tevatron and LHC studies, respectively, with the factorisation scale

Table 1 The selections applied in [6, 7] on the previously studied channels for Wγγ production at the Tevatron and LHC. Cuts were applied on the photon transverse momenta, p_T^γ, the charged lepton transverse momenta, p_T^l and pseudo-rapidity, $|\eta_l|$ and on the photon and charged lepton separations, ΔR. In addition, in order to suppress pho-

ton radiation from the final state charged lepton, the transverse mass of the (l, ν) system, $M_T(l, \nu)$, was required to satisfy $M_T(l, \nu) > 70$ GeV at the LHC and $65 < M_T(l, \nu) < 100$ GeV at the Tevatron. No energy smearing or efficiencies are applied

Collider	Process	p_T^e [GeV]	p_T^μ [GeV]	p_T^γ [GeV]	$|\eta_e|$	$|\eta_\mu|$	$\Delta R_{\gamma l}$	$\Delta R_{\gamma\gamma}$
Tevatron	$p\bar{p} \to e^- \nu\gamma\gamma$	>15	n/a	>15	<2.5	n/a	>0.7	>0.4
LHC	$pp \to l^\pm \nu\gamma\gamma$	>20	>25	>20	<2.5	<1.0	>0.4	>0.4

Table 2 Comparison of the previously published [6, 7] expected cross-sections for Wγγ production at the Tevatron and the LHC with the results obtained from the Baur and Lietti MCs. The selections at each collider are as defined in Table 1

Collider	Process	MC	Cross-section (fb)
Tevatron	$p\bar{p} \to e^- \nu\gamma\gamma$	Baur (published result)	0.50
		Baur (from MC provided)	0.50
LHC	$pp \to l^\pm \nu\gamma\gamma$	Lietti (published result)	1.76
		Lietti (from MC provided)	1.79
LHC	$pp \to e^- \nu\gamma\gamma$	Lietti (from MC provided)	0.546
		Baur (from MC modified for LHC)	0.672
		Lietti (from MC corrected)	0.675

in both cases being set equal to the parton centre of mass energy.

The prediction from each programme "as provided" was first verified against the corresponding published result. The Baur MC faithfully reproduced the reported cross-section for $p\bar{p} \to e^- \nu\gamma\gamma$ at the Tevatron, and likewise the Lietti MC for $pp \to l^\pm \nu\gamma\gamma$ at the LHC (see Table 2). However, when the Baur MC was modified to generate $pp \to e^- \nu\gamma\gamma$ events at the LHC, the expected cross-section was found to be about 25% higher than that obtained from the Lietti programme. Conversely, a similar modification of the Lietti MC for the generation of $p\bar{p}$ collisions at the Tevatron gave results comparable to those published. This discrepancy was due to the inclusion of only the $u\bar{d} \to l^+ \nu\gamma\gamma$ and $d\bar{u} \to l^- \nu\gamma\gamma$ contributions to the total cross-section within the Lietti MC. We have made a "corrected" version of this program by including the missing valence-sea quark terms, which make a significant contribution to the total cross-section at the LHC but play only a small role at the Tevatron.

3.2 Adaptation of a parton-level Monte Carlo for use with a showering and hadronisation generator
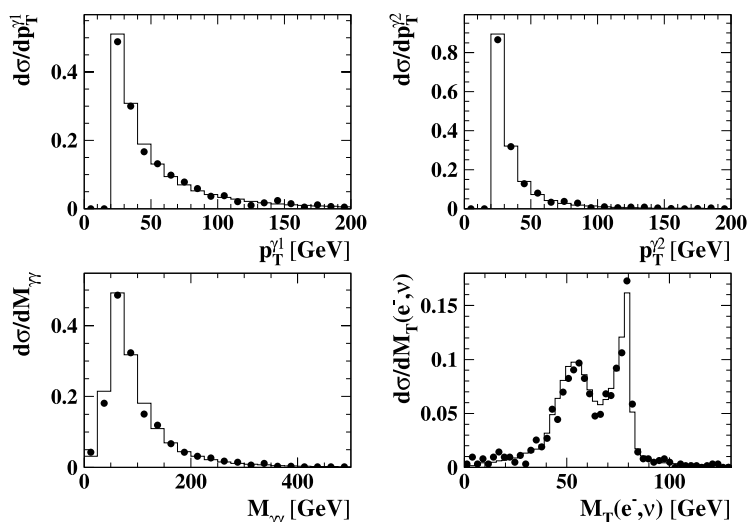
We have adapted the corrected Lietti MC for use with a showering and hadronisation generator (SHG) by adding a routine to write out events of unit weight in the Les Houches format [10]. This unweighting routine works in the

usual way, with each event being selected with a probability $P = w/w_{max}$, where w is the weight of the event and w_{max} is some maximum weight found from a large sample of events. In order to be able to label the incoming quarks in the event record, the weight w is expressed as the sum of the contributions from the different initial state $q\bar{q}$ combinations, in proportion to the parton distributions in that event, i.e. $w = w_{d\bar{u}} + w_{u\bar{d}} + \cdots$. For each unweighted event the initial state can therefore be assigned on a statistical basis and the incoming partons labelled accordingly.

We illustrate the correct functioning of the unweighting routine in Fig. 2. As mentioned above, the Baur MC generates only W⁻ events, meaning that the input $q\bar{q}$ mixture is always a combination of a down-type quark with an anti-up-type quark. Various distributions have been made using events with only these initial states selected from the full Lietti MC unweighted event record. In the figure these distributions are superimposed on those obtained directly from the Baur MC weighted events. The distributions are scaled according to the selected cross-sections from the two MCs. The result not only confirms the good agreement between the Baur and corrected Lietti programs, as already seen in Table 2, but also demonstrates the correct unweighting and labelling of events from the Lietti MC.

The adapted, corrected Lietti event generator, which we now name W2PHO [11], is available for download from the HepForge [12] website. This program was then employed in the subsequent work described here.

28

Eur. Phys. J. C (2009) 64: 25–33

4 Studying the WW$\gamma\gamma$ anomalous coupling in pp $\rightarrow$ l$^\pm v\gamma\gamma$ at the LHC

4.1 Generation and simulation of signal events

The W2PHO program was used to generate samples of
pp $\rightarrow$ l$^\pm v\gamma\gamma$ (l = e, v) events at the LHC centre of mass en-
ergy of $\sqrt{s} = 14$ TeV. The CTEQ5L structure functions were
used. The Les Houches format output files were provided as
input to Pythia version 6.4 [13] to perform the showering
and hadronisation. Subsequently, the response of a generic
LHC detector was simulated using the PGS program [14]
employing the default LHC detector description parameter
set. A minimal set of cuts were applied on the reconstructed
quantities to give the most inclusive selection within a likely
trigger acceptance:

– Transverse momenta of both photons, $p_T^\gamma > 15$ GeV.
– Transverse momentum charged lepton, $p_T^l > 25$ GeV.
– Missing transverse momentum, $p_T^{miss} > 25$ GeV.
– Pseudo-rapidity, η, of all charged leptons and photons sat-
  isfying $|\eta| < 2.5$.

Within these cuts an expected reconstructed cross-section of
8.6 fb was obtained, corresponding to around 260 SM events
in 30 fb^{-1} of integrated luminosity. It should be noted that
the cross-section increases approximately logarithmically as
the cut on the photon transverse momenta is reduced.

### 4.2 Observing and constraining the anomalous quartic gauge couplings

Since the effective Lagrangian terms for the AQGCs are
linear in the coupling constants β_0 and β_c the total cross-
section gains a quadratic dependence on each parameter,
with the squared term representing the pure anomalous
cross-section and the linear term the interference between

the SM and anomalous contributions. A simple counting
method could therefore be employed to compare the total
number of events observed with the number expected para-
metrised as a function of β_0 and β_c. Much greater sensitivity
can be obtained, however, by making use of the effect of any
AQGC contribution on the shapes of various distributions, as
shown in Fig. 3.

Of particular interest in Fig. 3 are the distributions of the
lepton-neutrino invariant mass, $M(l, v)$ and lepton-neutrino
transverse mass, $M_T(l, v)$. The AQGCs clearly contribute
to the $M(l, v)$ distribution exclusively at the W mass peak,
which is to be expected given the diagram of Fig. 1. Events
lying below this peak arise due to the final state photon ra-
diation from the charged lepton pulling the $M(l, v)$ mass
down below that of the W: these events are not part of
the pp $\rightarrow$ W($\rightarrow$ lv)$\gamma\gamma$ contribution to the total cross-section
where the sensitivity to the WW$\gamma\gamma$ vertex lies. Whilst the
$M(l, v)$ distribution cannot be obtained from experimen-
tal data the transverse mass distribution, $M_T(l, v)$ can be
used as an alternative: in the SM this distribution is also
peaked at M_W for events in which neither photon is emit-
ted from the charged lepton. The usual approach to isolate
the W($\rightarrow$ lv)$\gamma\gamma$ part of total cross-section is therefore to cut
away the region of $M_T(l, v)$ below, for example, 70 GeV, as
advocated in [6]. In Fig. 3, however, it can be seen in the
$M_T(l, v)$ distribution that the effect of the AQGC is not con-
fined to the region around M_W. The reason lies in the dis-
tribution of the transverse momentum of the (l, v) system,
$p_T(l, v)$: in the AQGC scenario, the system is boosted in the
transverse direction, which in turn distorts the shape of the
$M_T(l, v)$ distribution and increases the number of events in
the region below M_W [17]. As a result, cutting on $M_T(l, v)$
below the W mass gives an overall reduction in the sensitiv-
ity to any AQGC, and we do not apply such a cut here.

The bulk of the SM contribution lies in the region of low
photon transverse momenta, where the anomalous effects

Fig. 3 Distributions of the transverse momenta of the two photons, $p_T^{\gamma 1}$ and $p_T^{\gamma 2}$ (where $p_T^{\gamma 1} > p_T^{\gamma 2}$), the invariant mass of the two-photon system, $M_{\gamma\gamma}$, the transverse mass of the (l, ν) system, $M_T(l, \nu)$, the transverse momentum of the (l, ν) system, $p_T(l, \nu)$ and the invariant mass of the (l, ν) system, $M(l, \nu)$. The *solid lines* show the generator-level SM expectation, the *dashed line* is for the reconstructed events after processing in PGS (hence $M(l, \nu)$ is not available). The *dotted line* represents the generator-level expectation for $\beta_0 = 0.0001$ GeV^{-2}, which is about 0.02 of the LEP limit
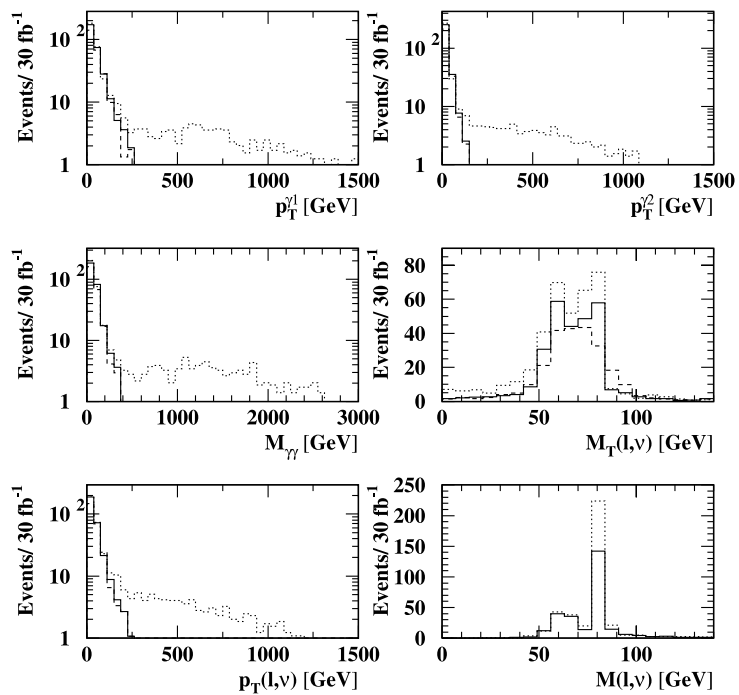
are also small, which could be cleanly cut away. However, whilst this would greatly improve the sensitivity of a counting method to the influence of the any AQGC, the method would remain critically dependent on an accurate prediction of the overall rate, on which there are many experimental (e.g. luminosity measurement) and theoretical (e.g. next to leading order effects) uncertainties. In this study we have applied a binned maximum likelihood method to the entire shape of various distributions, without discarding any of the SM data. The distribution most sensitive to any AQGC was identified by comparing the expected widths of the 95% confidence level intervals given a perfectly SM-like observation with 30 fb^{-1} of integrated luminosity. We found that the invariant mass of the two-photon system, $M_{\gamma\gamma}$, offered the optimal sensitivity. The statistical sensitivity achievable from the binned fit to the full $M_{\gamma\gamma}$ distribution is higher than that obtained from a counting method in which tight cuts are first applied to remove the SM background.

4.3 Simulation of background contribution

The dominant backgrounds are anticipated to be $W\gamma + \text{jets}$ and $W + \text{jets}$ events in which one or two jets are misidentified as photons. The probability for a jet to be misidentified in this way is given by $1/R_{\text{jet}}$ where R_{jet} is referred to as the jet rejection factor and is a property of the detector performance and reconstruction software. Since the cross sections for the background processes are several orders of magnitudes higher than that of the signal process, a high jet rejection factor is required if the background is not to dominate.

The expected background contribution arising from misidentified jets has been evaluated using Alpgen [15] samples of $W\gamma + 1\text{jet}$ and $W + 2\text{jet}$ events. The generated events were showered and hadronised in Pythia 6.4, employing the MLM parton matching scheme [16], and simulated in PGS. For the $W\gamma + 1\text{jet}$ events, an event was selected with weight $1/R_{\text{jet}}$ for any jet which, if relabelled as a photon, allowed the event to pass the signal selection cuts. For the $W + 2\text{jet}$ events, an event was selected with weight $1/R_{\text{jet}}^2$ for any pair of jets which, if relabelled as photons, allowed the event to pass the signal selection cuts.

The results are shown in Fig. 4, which presents the total signal plus background expectation assuming a jet rejection factor of 2000. It can be seen that the background contribution lies in the region populated by the SM signal process and is well separated from any possible AQGC signal.

4.4 Possible experimental limits on the anomalous couplings

To place confidence limits on the anomalous coupling parameters 10 000 samples of events were generated, the number of events in each sample being obtained from a Poisson distribution with a mean equal to the SM signal plus background expectation in 30 fb^{-1} of data. The results from one such "experiment" are shown superimposed in the plots of Fig. 4. For each sample, the 1-dimensional log-likelihood curves for β_0 and β_c were evaluated and from these the 95% confidence level limits on the parameters found. The couplings were varied independently with the parameter not under test fixed at its SM value (zero). These limits were then
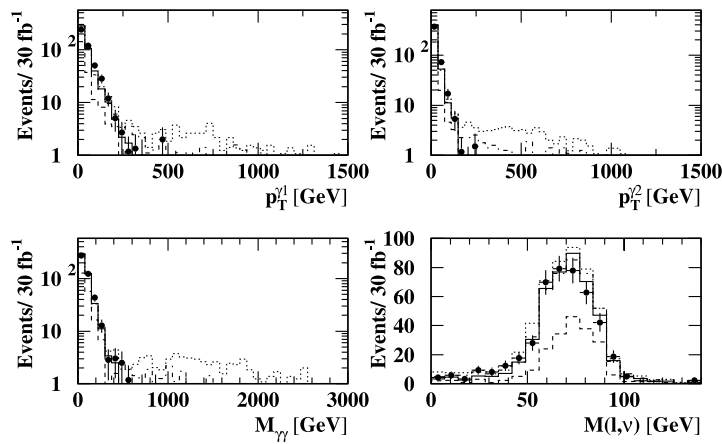
Fig. 4 Distributions of the transverse momenta of the two photons, $p_T^{\gamma 1}$ and $p_T^{\gamma 2}$ (where $p_T^{\gamma 1} > p_T^{\gamma 2}$), the invariant mass of the two-photon system, $M_{\gamma\gamma}$ and the transverse mass of the (l, ν) system, $M_T(l, \nu)$ assuming 30 fb^{-1} of integrated luminosity. The *solid lines* show the expected reconstructed SM signal plus background expectation. Of this, the *dashed line* shows the total background contribution from Wγ + jets and W + jets events assuming a jet rejection factor of 2000. The *dotted lines* and *dashed-dotted lines* are the expected reconstructed signal plus background expectation for $\beta_0 = 0.0001$ GeV^{-2} and $\beta_c = 0.0001$ GeV^{-2}, respectively. The points are for one LHC "experiment" according to the SM

Table 3 The expected 95% confidence level limits on the coupling parameters β_0 and β_c assuming 10, 30 and 100 fb^{-1} of integrated luminosity and assuming a jet rejection factor of 2000

	β_0	β_c
10 fb^{-1}	$(-2.98, 3.28) \times 10^{-5}$	$(-5.00, 4.92) \times 10^{-5}$
30 fb^{-1}	$(-1.85, 2.19) \times 10^{-5}$	$(-3.19, 3.21) \times 10^{-5}$
100 fb^{-1}	$(-1.16, 1.50) \times 10^{-5}$	$(-2.03, 2.14) \times 10^{-5}$

averaged over the 10 000 experiments to give the final results, which are presented in Table 3.

With 30 fb^{-1} of integrated luminosity, the limits are more than two orders of magnitude tighter than those available from LEP (OPAL). The limits obtained assuming 10 and 100 fb^{-1} of data are also shown for comparison.

To understand the effects of the background from the mis-identified jets, the confidence level limits for the 30 fb^{-1} case were also found as a function of the jet rejection factor. The results are shown in Fig. 5, where it can be seen that increasing the performance beyond 1000 does not significantly improve the limits.

4.5 Comparison to unitarity constraints

The effective Lagrangian terms generating the AQGCs spoil the gauge structure of the model, which can lead to unitarity violation at relatively low energies. To preserve unitarity up to higher energy scales, the conventional procedure is to modify the bare coupling parameters with an energy depen-
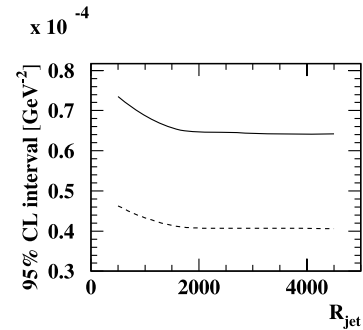

Fig. 5 The widths of the 95% confidence level intervals for β_0 (*solid line*) and β_c (*dashed line*) for 30 fb^{-1} of integrated luminosity as a function of the jet rejection factor

dent form factor. A typical choice is the generalised dipole form factor, which in this case would be applied as

$$\beta \to \left(1 + \frac{M_{\gamma\gamma}^2}{\Lambda_{FF}^2}\right)^{-n} \times \beta. \tag{1}$$

For values of $M_{\gamma\gamma}$ above the form factor scale, Λ_{FF}, this has the effect of pushing the AQGCs back down towards the SM prediction. The strength of this effect depends on the choice of n. For large n the form factor is effectively a cutoff on the effects of the anomalous couplings at Λ_{FF}, so that for $M_{\gamma\gamma} > \Lambda_{FF}$ any distribution becomes constrained to its SM expectation. The undesirable consequence of applying such a form factor is that any limits found will depend on the choices of n and Λ_{FF}.

The limits so far found refer to the bare couplings and cannot be assumed to be unitarity-safe. Rather than guaranteeing this by including some arbitrary, energy dependent

Fig. 6 The widths of the 95% confidence level intervals (*solid lines*) for β_0 and β_c as a function of the cutoff applied to the $M_{\gamma\gamma}$ invariant mass assuming 30 fb^{-1} of integrated luminosity. Superimposed (*dotted*) are the unitarity limits from (3) and (4). In each plot the region to the right of the *dotted line* is excluded by unitarity and above the *solid lines* by experiment
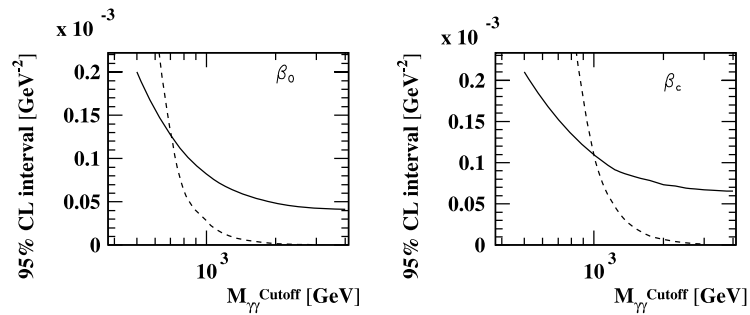
form factor correction, an alternative approach is taken, as advocated in [21], whereby the limits are evaluated as a function of a cutoff applied to the mass scale $M_{\gamma\gamma}$. This is plotted in Fig. 6: the experimental 95% confidence level intervals found for $M_{\gamma\gamma}^{\text{cutoff}} = 1$ TeV, for example, use only events for which $M_{\gamma\gamma}$ falls below this value. As the cutoff is increased, the experimental limits turn asymptotic, tending towards the values in Table 3: they do so at around 3 TeV, which is recognised as the ultimate reach of the experiment on the $M_{\gamma\gamma}$ scale.

To determine if the asymptotic limits are unitarity-safe, they can be compared to the unitarity constraints derived from the $2 \to 2$ inelastic scattering process $\gamma_1\gamma_2 \to W_1W_2$. The tightest energy dependent constraint arises from the J $= 0$ partial wave which can be written as [6]

$$\left(\frac{\alpha\beta M_{\gamma\gamma}^2}{16}\right)^2 \left(1 - \frac{4M_W^2}{M_{\gamma\gamma}^2}\right)^{\frac{1}{2}} \left(3 - \frac{M_{\gamma\gamma}^2}{M_W^2} + \frac{M_{\gamma\gamma}^4}{4M_W^4}\right) \le N, \quad (2)$$

where $M_{\gamma\gamma}$ is the invariant mass of the two photons and $N = \frac{1}{4}$ for $\beta = \beta_0$ and $N = 4$ for $\beta = \beta_c$. Defining $\Lambda_{\gamma\gamma}$ as the two-photon invariant mass scale at which unitarity is violated, for $\Lambda_{\gamma\gamma} \gg M_W$ the inequalities yield the following constant unitarity constraints on the couplings:

$$\beta_0 \le \frac{13.1 \text{ TeV}^2}{\Lambda_{\gamma\gamma}^4} \text{ TeV}^{-2}, \quad (3)$$

$$\beta_c \le \frac{52.4 \text{ TeV}^2}{\Lambda_{\gamma\gamma}^4} \text{ TeV}^{-2}. \quad (4)$$

These inequalities are shown superimposed in Fig. 6. In the region to the right of these dotted lines any new physics cannot be described by the effective Lagrangian theory. Assuming 30 fb^{-1} of integrated luminosity, the experimental limits at the reach of the machine lie well inside this region, and thus are weaker than those imposed by unitarity. The experiment will give tighter constraints on the couplings only up to $M_{\gamma\gamma} \sim 750$ GeV for β_0 and $M_{\gamma\gamma} \sim 1000$ GeV for β_c.

To obtain unitarity-safe limits, a form factor like (1) could be applied to the couplings with the scale Λ_{FF} set to 750 GeV and 1000 GeV for β_0 and β_c, respectively. The

limits as a function of $M_{\gamma\gamma}^{\text{cutoff}}$ would then turn asymptotic around these values, i.e. within the unitarity-allowed regions of the plots of Fig. 6. However, we have already noted that the effect of the form factor is to constrain the AQGC contribution to the SM prediction in the region where $M_{\gamma\gamma} > \Lambda_{\text{FF}}$. It would therefore make no sense to use any data collected in this region to measure the AQGCs; any effects would be highly overestimated in overcoming the suppression of the form factors. Consequently, it has been argued that the scale chosen for Λ_{FF} should not be within the reach of the experiment [21]. Applying a generalised dipole form factor like (1) is therefore an unsuitable way to ensure unitarity here, and instead limits on the bare couplings should be found using a restricted range of the $M_{\gamma\gamma}$ distribution.

It can be seen in Fig. 6 that the experimental limits at the edge of the unitarity-allowed region of the $(M_{\gamma\gamma}, \beta)$ plane are weakened by approximately a factor two compared to the asymptotic limits, and so will remain around two orders of magnitude stricter than those available from LEP (OPAL).

5 Observation of the radiation zero in W$\gamma\gamma$ events at the LHC

At the Born level in the SM the amplitude for $q\bar{q}' \to W^{\pm}\gamma\gamma$ exhibits a cancellation for $\cos\theta^{\star} = \mp\frac{1}{3}$ when the two photons are collinear, where $\theta^{\star}$ is the angle between the incoming quark and the W boson in the parton centre of mass frame [18–20]. It has been shown that this so called *radiation zero* only gradually vanishes as the opening angle of the photons is increased, and may be observed experimentally as a "dip" in the distribution of $\Delta\eta = \eta_{\gamma\gamma} - \eta_l$, where $\eta_{\gamma\gamma}$ and η_l are the pseudo-rapidities of the two-photon system and the charged lepton, respectively [7].

At a pp collider such as the LHC, the symmetric beams mask the asymmetry of the radiation zero and the dip in $\Delta\eta$ occurs at zero. However, it has been suggested [21] that the distribution may be "signed" according to the longitudinal direction of the final state system. Since the quark is statistically most likely to come from the valence distribution in the proton, whereas the anti-quark has to come from the sea
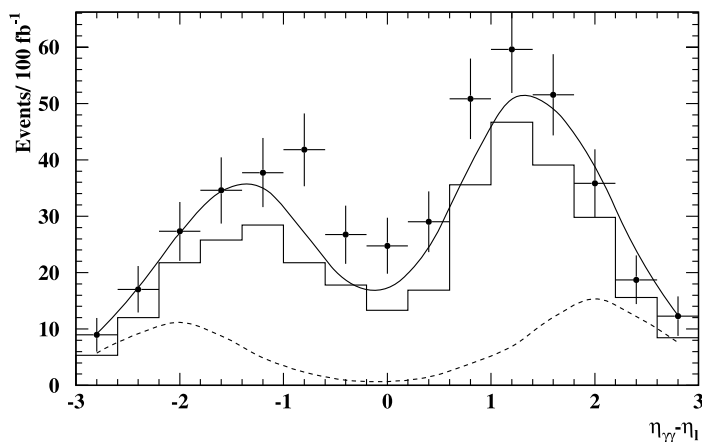
32

Eur. Phys. J. C (2009) 64: 25–33

Fig. 7 The pseudo-rapidity separation of the charged lepton from the two-photon system for Wγγ production at the LHC, showing the radiation zero "dip". The kinematic cuts are as described in Sect. 4.1, with the cut on the charged lepton and photon separations hardened to $\Delta R > 0.7$ and an additional requirement imposed on the (l, ν) transverse mass of $M_T(l, \nu) > 70$ GeV. The *solid curve* shows the generator-level expectation for the "signed distribution", the histogram is the signal after simulation in PGS and the points are the signal plus background assuming a jet rejection factor of 4000. The *dotted line* is the generator-level expectation after additionally requiring that the opening angle of the two photons in the Wγγ centre of mass frame satisfies $\cos(\theta^*_{\gamma\gamma}) > 0$

distribution, the quark will tend to carry a larger momentum fraction than the anti-quark and the lγγ system will most likely be boosted in the quark direction. The longitudinal direction of the lγγ system can therefore be evaluated and if found to be in the backward direction the sign of the $\Delta\eta$ distribution reversed. To take account of the inherent sign difference between the W$^+$ and W$^-$ cases the sign of $\Delta\eta$ is also reversed for the W$^-$ events. This signing maintains the asymmetry of the radiation zero, as can be seen in Fig. 7.

For the plot in Fig. 7 the event selection of Sect. 4.1 has been tightened by imposing a cut on the charged lepton and photon separations of $\Delta R > 0.7$ and on the (l, ν) transverse mass of $M_T(l, \nu) > 70$ GeV. These cuts reduce the effects of photon radiation in the directions of the final state charged lepton and initial state quarks, respectively, which would otherwise obscure the radiation zero. The background contribution from the mis-identified jets also acts to fills in the dip, and a tighter jet rejection factor of 4000 is therefore used. With these additional constraints the dip is clearly visible in 100 fb^{-1} integrated luminosity.

Since the exact cancellation requires that the two photons be collinear, it has been suggested [7] that the radiation zero can be enhanced by cutting on the two-photon opening angle, $\cos(\theta_{\gamma\gamma})$. Contrary to what was reported in [7], however, it was found here that such a cut is effective only if applied in the centre of mass system. Boosting to the centre of mass frame requires the knowledge of the missing longitudinal momentum, which can be reconstructed with a twofold ambiguity if it is assumed that the missing transverse momentum belongs exclusively to the neutrino and that the W is produced on-shell. Experimentally it is not possible to determine which of the two solutions for the missing longi-

tudinal momentum is the correct one, but statistically it is most likely to be the one which gives the smallest mass to the Wγγ system. Using this "minimum mass solution", the events can be boosted to the centre of mass frame where the requirement that the two photons are in the same hemisphere is imposed, i.e. $\cos(\theta^*_{\gamma\gamma}) > 0$. Making the boost and applying this cut can be seen to increase the significance of the radiation zero, as shown by the dashed curve in Fig. 7, at the expense of a significant loss of signal events.

It is worth noting that the radiation zero is sensitive to the AQGCs, which act to fill in the dip. However, the two-photon invariant mass was found to be a more sensitive distribution and the radiation zero will anyway be filled in by many other effects, such as background events and next to leading order (NLO) QCD contributions. The order α_s QCD corrections involve both the virtual and radiative gluon corrections to the $q\bar{q}' \rightarrow W\gamma\gamma$ reaction and the quark–gluon initiated processes $qg \rightarrow W\gamma\gamma q'$ and $g\bar{q}' \rightarrow W\gamma\gamma q$. As in the Wγ case [22], in order to preserve the visibility of the radiation zero we expect that a jet veto will be required to suppress these quark–gluon initiated processes that do not possess a radiation zero, and which are otherwise dominant at LHC energies.

6 Summary and conclusions

Probing the quartic gauge boson couplings represents an important test of the non-Abelian structure of the Standard Model, and anomalous contributions to these couplings may indicate the presence of new physics, possibly in the important electroweak symmetry breaking sector. The pp→ l$^\pm$νγγ

(l = l, μ) process of Wγγ triboson production offers an interesting starting point for the study of AQGCs at the LHC. Under the most inclusive event selection, the cross section for this process is expected to be 8.6 fb, which will yield around 260 events with an integrated luminosity of 30 fb^{-1}.

After testing various distributions with a binned maximum likelihood fit, we suggest that the two-photon invariant mass will offer the best sensitivity to the anomalous coupling parameters β_0 and β_c associated with the WWγγ vertex. The experimental sensitivity to the anomalous couplings reaches into the region of the $(M_{\gamma\gamma}, \beta)$ plane where the effective Lagrangian theory breaks down, and a cutoff must be applied to the $M_{\gamma\gamma}$ scale to ensure unitarity conservation. Beyond this cutoff, the new physics would be directly visible in other channels. Working below the cutoff, the expected limits on the bare couplings remain around two orders of magnitude tighter than those currently available from LEP.

When studying the pp $\rightarrow$ l$^{\pm}$νγγ events, it is interesting also to plot the "signed" distribution of $\Delta\eta = \eta_{\gamma\gamma} - \eta_l$ which should reveal the radiation zero present in the SM amplitude. This can be enhanced by cutting on the opening angle of the two photons in the centre of mass system, but will require more than 30 fb^{-1} of data and the use of a jet veto to be experimentally observable.

References

1. S. Godfrey, in *Proceedings of the International Symposium on Vector Boson Self-Interactions*, UCLA, USA, 1995. hep-ph/950525
2. G. Bélanger, F. Boudjema, Phys. Lett. B **288**, 201 (1992)
3. W.J. Stirling, A. Werthenbach, Eur. Phys. J. C **14**, 103 (2000)
4. G. Bélanger et al., Eur. Phys. J. C **13**, 283 (2000)
5. G. Abbiendi et al. (OPAL Collaboration), Phys. Rev. D **70**, 032005 (2004)
6. O.J.P. Eboli, M.C. Gonzalez-Garcia, S.M. Lietti, S.F. Novaes, Phys. Rev. D **63**, 075008 (2001)
7. U. Baur, T. Han, N. Kauer, R. Sobey, D. Zeppenfeld, Phys. Rev. D **56**, 140 (1997)
8. T. Stelzer, W.F. Long, Comput. Phys. Commun. **81**, 357 (1994)
9. G.P. Lepage, J. Comput. Phys. **27**, 192 (1978)
10. E. Boos et al., in *Proceedings of the Workshop on Physics at TeV Colliders*, Les Houches, France, 2001. hep-ph/0609017
11. http://projects.hepforge.org/w2pho/
12. J.M. Butterworth et al., in *Proceedings of Computing in High-Energy Physics (CHEP '04)*, Interlaken, Switzerland, 2004. hep-ph/041213. http://www.cedar.ac.uk
13. T. Sjostrand, S. Mrenna, P. Skands, J. High Energy Phys. **05**, 26 (2006)
14. J. Conway, http://www.physics.ucdavis.edu/~conway/research/software/pgs/pgs4-general.htm
15. M.L. Mangano, M. Moretti, F. Piccinini, R. Pittau, A.D. Polosa, J. High Energy Phys. **0307**, 001 (2003)
16. M.L. Mangano, M. Moretti, F. Piccinini, M. Treccani, J. High Energy Phys. **01**, 013 (2007)
17. J. Smith, W.L. van Neerven, J.A.M. Vermaseren, Phys. Rev. Lett. **50**, 1738 (1983)
18. S.J. Brodsky, R.W. Brown, Phys. Rev. Lett. **49**, 966 (1982)
19. R.W. Brown, K.L. Kowalski, S.J. Brodsky, Phys. Rev. D **28**, 624 (1983)
20. R.W. Brown, K.L. Kowalski, Phys. Rev. D **29**, 123 (1984)
21. M. Dobbs, in *Proceedings of the 15th International Topical Conference on Hadron Collider Physics (HCP2004)*, Michigan State University, USA, 2004. hep-ph/0506174
22. U. Baur, S. Errede, G. Landsberg, Phys. Rev. D **50**, 1917 (1994)